Brain region and sex-dependent heterogeneity of PUFA/oxylipin profile, microglia morphology and their relationship

Geertsema, J.; Franßen, M.A.; Barban, F.; Šarauskytė, L.; Giera, M.; Kooij, G.; Korosi, A

DOI
10.1016/j.plefa.2024.102662

Publication date
2025

Document Version
Final published version

Published in
Prostaglandins, leukotrienes and essential fatty acids

Prostaglandins, Leukotrienes and Essential Fatty Acids 204 (2025) 102662

Contents lists available at ScienceDirect

Prostaglandins, Leukotrienes and Essential Fatty Acids

journal homepage: www.elsevier.com/locate/plefa

Original research article

Brain region and sex-dependent heterogeneity of PUFA/oxylipin profile, microglia morphology and their relationship

J. Geertsema [a], M.A. Franßen [b], F. Barban [a], L. Šarauskytė [a], M. Giera [c], G. Kooij [b], A Korosi [a,*]

[a] Center for Neuroscience, Swammerdam Institute for Life Sciences, University of Amsterdam, Amsterdam, , Netherlands
[b] Department of Molecular Cell Biology and Immunology, Amsterdam Neuroscience, MS Center Amsterdam, Amsterdam UMC, Vrije Universiteit Amsterdam, Amsterdam, , Netherlands
[c] Leiden University Medical Center, Center for Proteomics & Metabolomics, Leiden, Netherlands

ARTICLE INFO

Keywords:
Hypothalamus
Hippocampus
Microglia
PUFA
Oxylipins

ABSTRACT

Lipid dyshomeostasis and neuroinflammation are key hallmarks of neuropsychiatric and neurodegenerative disorders, including major depressive disorder and Alzheimer's disease. In particular, polyunsaturated fatty acids (PUFAs) and their derivatives called oxylipins gained specific interest in this context, especially considering their capacity to orchestrate neuroinflammatory responses via direct modulation of microglia. The hippocampus and hypothalamus are crucial brain regions for regulating mood and cognition that are implicated in a variety of neuropsychiatric and neurodegenerative disorders and there is ample evidence for the sex-bias in risks for the development as well as sex-bias in the presentation of such psychiatric diseases, including the neuroinflammatory response. To better understand the local PUFA/oxylipin profiles and microglia responses in disease, we here assessed their brain region and sex-dependent profiles in homeostatic brains. In 2-month-old male and female mice, we measured non-esterified (free) PUFA/oxylipin profiles using liquid chromatography-tandem mass spectrometry and characterized microglia morphology via immunohistochemistry. The hypothalamus and hippocampus exhibit a different free PUFA/oxylipin profile, independent of sex. The hippocampus was characterized by a higher density of complex Iba1^{+} microglial cells than the hypothalamus, without sex effects. Hypothalamic microglial morphology correlated more strongly with free PUFA- and oxylipin species than hippocampal microglia, correlating with species from both the N-3 and N-6 PUFA metabolization pathways, while hippocampal microglial parameters correlated only with N-6 pathway-related species. Our findings provide a basis for future studies to investigate the relationship between PUFAs, their derivatives and neuroinflammation in the context of diseases.

1. Introduction

Brain lipid dyshomeostasis and neuroinflammation are emerging hallmarks in neuropsychiatric and neurodegenerative disorders (including depression and Alzheimer's disease) [1–4]. Polyunsaturated fatty acids (PUFAs) and their derivatives called oxylipin species have gained attention in this context [3,5]. PUFAs are essential fatty acids that are crucial for membrane structure and fluidity, and are necessary for normal brain functioning and development [6]. In fact, PUFA derivatives, the highly biologically active oxylipins [7], are important

Abbreviations: AA, arachidonic acid; ABA, atlas-based analysis; AdA, adrenic acid; ALA, α-linolenic acid; ARC, arcuate nucleus; BSA, bovine albumin serum; CA, Cornu Ammonis; DG, dentate gyrus; DHA, docosahexaenoic acid; DM, dorsomedial hypothalamus; DPA, docosapentaenoic acid; FDR, false discovery rate; HCPC, hierarchical clustering on principal components; HEPE, hydroxy-eicosapentaenoic acid; HETE, hydroxyeicosatetraenoic acid; HoDE, hydroxyoctadecadienoic acid; HPLC-MS/MS, high-pressure liquid chromatography-mass spectrometry; KETE, ketoeicosatetraenoic acid; LA, linolenic acid; LH, lateral hypothalamus; LM, lipid mediators; LT, leukotriene; Iba1, ionized calcium binding adaptor molecule 1; MeOH, methanol; N, omega; P, postnatal day; PB, phosphate buffer; PBS, phosphate buffered saline; PCA, principal component analysis; PFA, paraformaldehyde; PG, prostaglandin; PLS-DA, partial least squares discriminant analysis; PUFA, polyunsaturated fatty acid; PVN, paraventricular nucleus; ROI, region of interest; RT, room temperature; SD, standard deviation; SPE, solid phase extraction; TB, tris buffer; TBS, tris-buffered saline; TNF, tumor necrosis factor; VIP, variable importance projection; VMH, ventromedial hypothalamus.

* Corresponding author at: Brain Plasticity group, Swammerdam Institute for Life Sciences (SILS), University of Amsterdam, Science Park 904, 1012 WX Amsterdam, The Netherlands.
E-mail address: a.korosi@uva.nl (A. Korosi).

https://doi.org/10.1016/j.plefa.2024.102662
Received 20 September 2024; Received in revised form 6 December 2024; Accepted 10 December 2024
Available online 16 December 2024

mediators of pro-inflammatory as well as inflammation-resolution processes [3,8,9]. The two most common sub-classes (omega (N)−3 PUFAs and N-6 PUFAs) and their derivatives are amongst others able to modulate microglia directly, by modulating their motility, phagocytosis and cytokine release [8,9].

The hippocampus and the hypothalamus are key brain regions for regulating mood and cognition and their dysregulations has been implicated in neuropsychiatric and neurodegenerative disorders [10]. In addition, there is ample evidence for the sexual dimorphism in risks to develop and presentations of such neuropsychiatric and neurodegenerative disorders [11] as well as in the neuroinflammatory system [12–15]. However, in order to deepen our insight into the role of free PUFA/oxylipin profile and microglia in disease, we first need to understand their brain region and sex-dependent profiles as well as to explore how they relate to each other in the homeostatic brain. There is initial evidence suggesting a brain region and/or sex heterogeneity in abundance of free PUFA- and oxylipin species within the brain. For example, the cerebellum, the hypothalamus, the cortex and the hippocampus exhibited a brain region-specific eicosanoid profile in 16-week--old male mice [16]. However, in 2-month-old male rats, while free PUFA/oxylipin profiles were not different at baseline in hippocampus, cortex, the cerebellum and the brainstem, specifically the linoleic acid (LA)-derived free PUFA- and oxylipin species were differentially present in these brain regions following ischemia [17]. Concerning sex differences, in 1-day-old rat pup brains, no sex differences were found between the free PUFA- and oxylipin species [18], while mice at the age of 4-months [19] or 32 weeks [20] exhibited an increased 5-hydroxyeicosatetraenoic acid (HETE) and 5-hydroxy-eicosapentaenoic acid (HEPE) in the cerebellum [19] and higher levels of 9, 11 and 15-HETE in a whole hemisphere in males compared to females [20], respectively.

However, i) if and how the free PUFA/oxylipin profile might differ specifically between hippocampus and hypothalamus, ii) between sexes and iii) how such profiles relate to specific aspects of microglia morphology is currently not known. Addressing these aspects is the focus of our study and obtained findings will enhance our understanding of free PUFA- and oxylipin species and their possible relationship with microglia within the homeostatic brain, while forming the foundation for future studies that seek to elucidate the role of PUFA metabolism and neuroinflammation in the context of psychiatric diseases.

2. Materials and methods

2.1. Animals and breeding

Wildtype C57BL6/J mice were bred in-house to control for the perinatal period. Pregnant females were single-housed in a cage with standard bedding and nesting material. Every 24 h, before 10:00 a.m., the birth of pups was monitored. When litters were born before 10:00 a.m., the previous day was assigned postnatal day (P)0. Animals were weaned at P21–23 and housed in standard housing conditions (sawdust bedding, paper straw cage enrichment, temperature 20–22°C, humidity 40–60 %, standard 12–12 h light/dark schedule lights on at 8:00 a.m. and water and food (Special Diets Services: CRM(P), product code: 801,722) ad libitum) with maximum 3 littermates of the same sex.

All experimental procedures were executed according to the Dutch national law and European Union directive 2010/63/EU on animal experiments and were approved by the animal welfare committee of the University of Amsterdam.

2.2. Tissue collection

At P59–61, mice were sacrificed via an intraperitoneal Euthasol injection (100 mg/kg, AST Farma) followed by transcardial saline (0.09 % NaCl in MilliQ water) perfusion. After perfusion, the brains of mice were split in hemispheres. From the left hemisphere, the hippocampus and hypothalamus were dissected and used for targeted high-pressure liquid chromatography-tandem mass spectrometry (HPLC-MS/MS)-based lipidomics and kept at −80°C. The right hemisphere was dropped in 4 % paraformaldehyde (PFA), post-fixed for 24 h and then kept at 4°C in 0.01 M phosphate buffer (PB) (pH 7.4) containing 0.01 % sodium azide until further processing. The PFA-fixed hemisphere was first put in a solution of 15 % sucrose followed by one of 30 % sucrose in 0.1 M PB for cryopreservation. Then, the hemisphere was sliced into 40 μm thick sections in 6 parallel series on a freezing microtome and kept in antifreeze solution (30 % ethylene glycol + 20 % glycerol + and 50 % 0.05 M phosphate-buffered saline (PBS)) and kept at −20°C until further use. For an overview of the processing of all samples, see Fig. 1A.

2.3. Targeted LC-MSMS for the detection of non-esterified PUFA- and oxylipin species

2.3.1. Sample processing

Sample preparation (Male hippocampus: $n = 6$, female hippocampus: $n = 7$, male hypothalamus: $n = 4$, female hypothalamus = 6, from 2 to 3 litters) and measurement was in accordance with a previously described method [21], with the adaption that 2-propanol was used for homogenization. Hypothalamic and hippocampal tissues were weighed and homogenized in 2-propanol (10 mg/mL for hypothalami, 40 mg/mL for hippocampi) using a bullet blender and metal beads. 100 μL of hypothalamic homogenates were extracted and combined with 500 μL ice-cold methanol (MeOH, Sigma, Saint Louis, MO, USA), 200 μL ultra-grade water (Sigma Aldrich, Schnelldorf, Germany), and 4 μL internal standard solution (deuterated lipid mediators: leukotriene (LT) B4-d4 (50 ng/mL), (±) 15-HETE-d8 (50 ng/mL), prostaglandin (PG) E2-d4 (50 ng/mL), 8-isoPGF2α-d4 (100 ng/mL), docosahexaenoic acid (DHA)-d5 (500 ng/mL), and 14(15)-epoxy-eicosatrienoic acid-d11 (50 ng/mL) (Cayman Chemical, Ann Arbor, MI, USA)). For hippocampal homogenates, 150 μL was extracted with 750 μL ice-cold MeOH, 300 μL ultra-grade water, and 4 μL internal standard solution Samples were incubated for 20 min at −20°C, then centrifuged at 16,100 x g and 4°C. Supernatants were transferred to 15 mL tubes, diluted with 7.5 mL H_2O, and acidified to pH 3.5 with 10 % formic acid (84,865.180, VWR). Solid-phase extraction with C-18 cartridges (Sep-Pak, Vac3 3cc (200 mg), Waters, MA, USA) was used to extract lipids. Samples were cleaned with H_2O and n-hexane (VWR), eluted with methylformate (259,705, Honeywell-Riedel de Haën), and dried at 40°C under nitrogen. Dried samples were reconstituted in 80 μL MeOH and 120 μL H_2O, then transferred to deactivated glass inserts. 40 μL of the solution was injected into an HPLC system.

The HPLC system (Shimadzu) used a C18 column with a C8 precolumn. Column temperature was maintained at 50°C. Lipids were separated by a linear gradient between solvent A (H_2O with 0.01 % acetic acid) and solvent B (MeOH with 0.01 % acetic acid) at 0.4 mL/min. A Sciex Qtrap 6500 tandem mass spectrometer in negative electrospray ionization mode was used to detect individual PUFA and oxylipins, as listed in Supplementary Table 2. Peak identification was performed using Sciex Analyst® Software. Absolute concentrations were determined for 27 lipid species using external calibration curves; relative abundance was defined relative to the internal standard (area ratio) for other lipids. This method allowed for the detection of non-esterified (free) PUFA and oxylipin species.

2.3.2. Data pre-processing

Subsequently, components were only taken along for further analysis if present in at least 80 % samples within one group [22]. Based on this rule, we excluded one component, ending with 21 components in total. Finally, remaining missing values were imputed using a Gibbs sampler based left-censored imputation method described by Wei et al. [23]. Area ratio values were normalized to the sample amount.

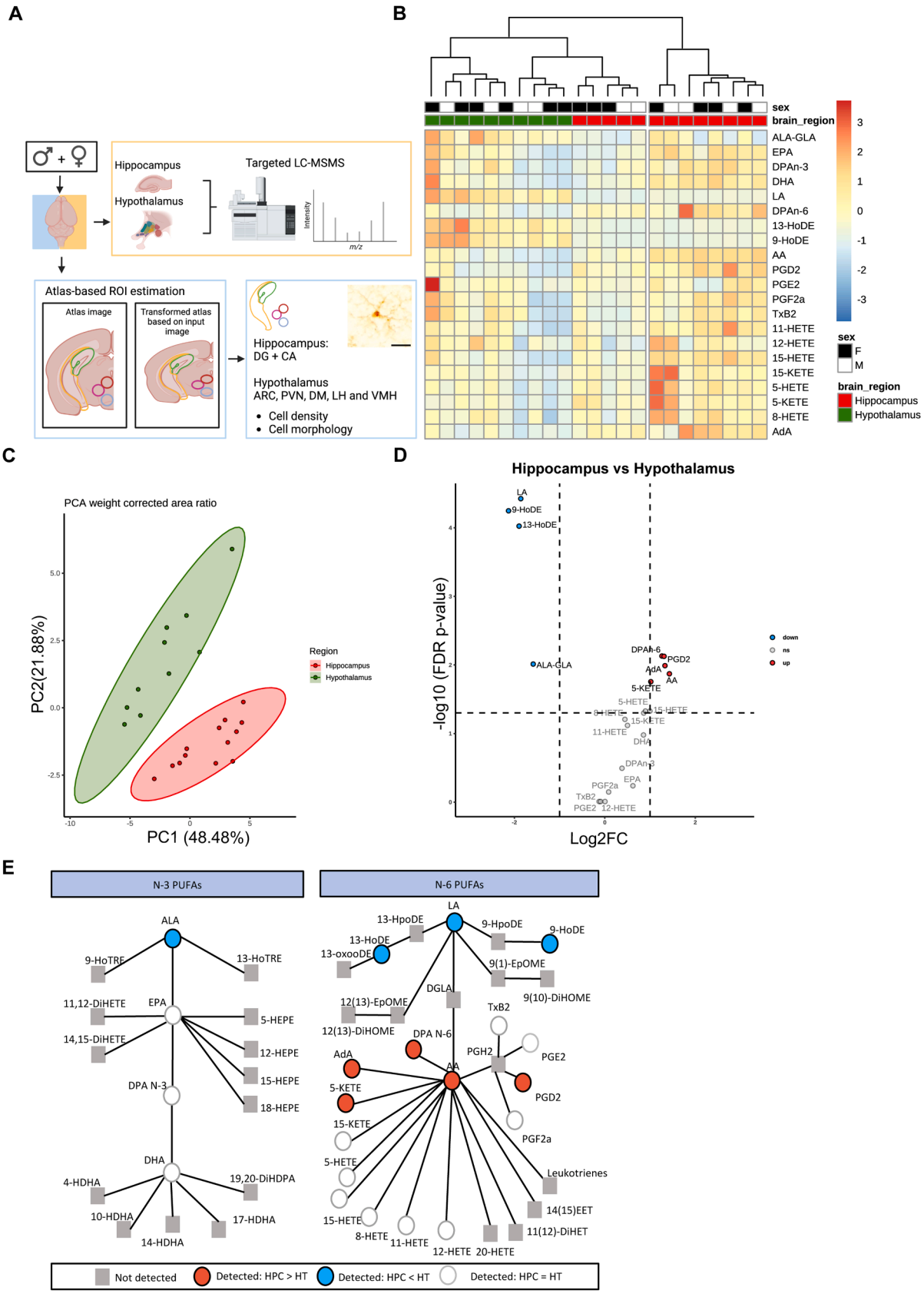

(caption on next page)

Fig. 1. Non-esterified PUFA- and oxylipin profile in the hippocampus and the hypothalamus A) Workflow of the experiment. Males and females (P60) were sacrificed by saline perfusion and one hemisphere was selected for free PUFA- and oxylipin profiling, while the other was used for immunohistochemical staining of Iba1. B) Heatmap with hierarchical cluster analysis (Euclidean distance) showing the separation of animals (x-axis) by brain region but not sex for the various lipid mediators. C) Principal Component Analysis (PCA) Plot of free PUFA- and oxylipin species of hypothalamic and hippocampal samples. D) Volcano plots showing the log2 fold change of free PUFA- and oxylipin species between the hippocampal- and hypothalamic tissue. The level of significance is indicated on the y-axis as –log10 (FDR *p*-value). E) Figure representing all free PUFA- and oxylipin species in their respective N-3 or N-6 pathway. Symbols and colors are indicative of the effect. Square is not detected; Circle is detected; Red circle means detected in higher abundance in the hippocampus compared to the hypothalamus; Blue circle means detected in lower abundance in the hippocampus compared to the hypothalamus and a white circle represents those which were detected in similar abundance in the hippocampus and the hypothalamus.

2.4. Immunohistochemistry

Free-floating sections (Male hippocampus: $n = 8$, female hippocampus: $n = 8$, male hypothalamus: $n = 8$, female hypothalamus= 8, from 3 litters) were washed (3 × 5 min) in 0.05 M tris-buffered saline (TBS) (pH 7.6), followed incubation in 0.3 % H2O2 in TBS for 15 min. This was followed by washing in TBS (3 × 5 min). Then the sections were transferred in a blocking solution (1 % bovine albumin serum (BSA) + 0.3 % triton in TBS) for 30 min. The slices were incubated with primary antibody (Rabbit anti-Ionized calcium binding adaptor molecule 1 (Iba1) 1:1000, WAKO, 019–19,741) at room temperature (RT) in blocking solution, followed by an overnight incubation at 4°C. The day after, samples were washed in 0.05 M TBS + 0.3 % triton (3 × 5 min). Then, sections were incubated with a secondary antibody (Biotinylated, goat anti-rabbit, 1:500, Vector Laboratories, BA-1000–1.5) for 2 h at RT. Sections were washed in 0.05 M TBS (3 × 5 min) and incubated in avidin-biotin complex in 0.05 M TBS for 90 min afterwards (Vectastain Elite ABC Elite kit, 1:800 for each component, Vector Laboratories, PK-6100) After washing 5 times (4 × 5 min with 0.05 TBS followed by 5 min in 0.05 M tris buffer (TB)), sections were incubated with 0.5 mg/mL 3,3′-diaminobenzidine (Sigma-Aldrich, D12384) in 0.05 M TB (pH = 7.6) with 0.1 % H_2O_2 in 0.5 M TB. Sections were fast washed three times in TB, followed by washes in TB (2 × 5 min). Sections were mounted, dehydrated and covered with Entellan (Sigma-Aldrich, 1.07960)

2.5. Image analysis

Using the AxioScanZ1, the microscope slides were scanned with a 40x objective. Images were converted to 8-bit images, followed by different steps taken for the hippocampus and hypothalamus for the processing of images for coverage and cell density analysis.

2.5.1. Hippocampus

To ensure representative analyses of the hippocampus, we took six dorso-ventral sections located between bregma points −1.22 to −3.64. The cornu ammonis (CA) and the dentate gyrus (DG) were traced using ImageJ and saved as regions of interest (ROI) for further processing.

2.5.2. Hypothalamus

The hypothalamus is a heterogeneous structure, with unclearly demarcated regions. For this reason, atlas-based analysis (ABA) [24] was used to draw ROIs in the hypothalamus.

2.5.3. Atlas-based estimation of ROIs

The Warp Image plugin was used to increase overlay accuracy between imaged sections and the atlas diagrams. Diagrams from the atlas containing either of the following five hypothalamic ROI: Arcuate nucleus (ARC), Paraventricular nucleus (PVN), Dorsomedial hypothalamus (DM), Lateral hypothalamus (LH), Ventromedial hypothalamus (VMH) were used. Landmarks (such as ventricles and commissural fibers) are used as orientation points, used to alter the atlas image (moving image) to align more accurately with the section image (fixed image). The atlas was transformed based on homography transformation using the semi-automated ABA [24]. After overlaying the matched atlas onto the section sample on the microscopic image, each of the regions was outlined in ImageJ for each image (4 per animal) and saved as an ROI.

2.6. Quantification of Iba1 coverage and cell density

Quantification of Iba1 staining was done by an experimenter blinded for sex. A fixed threshold was determined for all hypothalamic and hippocampal images to determine the percentage of immunoreactive stained area (coverage) in the respective regions. The total thresholded signal of each image was added up and was divided by the total area of ROIs, producing a single coverage datapoint per animal. Data are presented as percentage coverage.

For cell density analysis, within the same ROIs used for the coverage analysis, Iba1$^+$cells were manually counted by an experimenter blind for animal sex. The amount of Iba1$^+$cells in each ROI was added up and divided by the area of those ROIs. Data are presented as Iba1$^+$cells per surface area.

2.7. Morphometric analysis

1920 representative single Iba1$^+$cells were selected from whole slide scans by an experimenter blind for animal sex. For the hippocampus, we extracted 25 cells per region (CA and DG) per animal, derived from both dorsal and ventral sections representing the full hippocampus. For the hypothalamus we extracted cells based on the size of the region (ARC and PVN: 5 cells/animal; DM, VMH, LH = 20 cells/animal), derived from both dorsal and ventral slices of that region representing the full dorso-ventral axis of the hypothalamus.

The single-cell images were processed to cell silhouette images by local thresholding and subsequently morphometric parameters were extracted as described before [25]. With the use of these parameters, a hierarchical clustering on principal components (HCPC) was conducted on all cells to identify 6 Iba1$^+$ morphotypes and to observe how they compared between different males and females in different brain regions.

2.8. Statistical analysis

2.8.1. Free PUFA- and oxylipin species measurements

Group differences were tested using the unpaired Wilcoxon rank-sum test ($\alpha = 0.05$) with false discovery rate (FDR) correction, reporting both adjusted and non-adjusted p-values. Plots and statistics were generated in R (R Foundation for Statistical Computing, Version 2023.12.0) using rstatix, pheatmap, and ggplot2. Multivariate analysis was conducted with mixOmics, with data centered and unit variance scaled.

2.8.2. Microglial parameters

Data were analyzed using R (version 4.2.1) and bar graphs were graphed in Graphpad Prism 10. Data are expressed as mean ± standard deviation (SD). α was set at 0.05, and data were considered statistically significant when $p < 0.05$. Data points that were outside the 1.5 interquartile range were excluded from analysis as outliers. Assumptions of parametric analysis were tested using the Shapiro-Wilk normality test and Levene's test for homogeneity of variance. When taking brain region and sex as independent factors, e.g. for the data of Iba1$^+$cell density, Iba1 coverage, and cell complexity were analyzed with a Two-way ANOVA. Multiple cells from one animal were used, so we averaged all datapoints from Iba1$^+$cells deriving from the same animal, producing a single data point per animal.

2.8.3. Correlation between microglial parameters and free PUFA- and oxylipin species

The morphology parameters that were obtained for microglial morphotyping, were correlated with free PUFA- and oxylipin species. Correlations were calculated based on complete pairwise cases. As it is an explorative study, data presented here are not FDR-corrected. Correlation coefficients were tested against critical values on a two-tailed distribution ($\alpha = 0.05$). (Supplementary Tables 1 and 2 (Hippocampus: Supplementary Table 1; Hypothalamus: Supplementary Table 2).

3. Results

3.1. The hippocampus and the hypothalamus display a differential free PUFA/oxylipin profile independent of sex

To assess potential brain region- and sex-dependence of local free PUFA/oxylipin profiles, free PUFA- and oxylipin species were detected using their relative retention times and thereafter, we performed a Euclidean clustering visualized by a heatmap Fig. 1B. Hippocampal tissue seems to in general express more PUFAs and oxylipin species, compared to the hypothalamus and their free PUFA/oxylipin profiles were separated, independent of sex, which was also confirmed by a signed rank Wilcoxon test (See also Supplementary Table 3). In the following steps, therefore, samples from both sexes were pooled. When performing a principal component analysis (PCA), a clear separation was seen between hippocampus and hypothalamus, (Fig. 1C). The strongest contributors in dimension 1 were arachidonic acid (AA), 11-HETE, 15-HETE, and LA in dimension 2 (Supplementary fig. 1A). A partial least squares discriminant analysis (PLS-DA) was subsequently performed for a targeted discrimination of the brain areas based on free PUFA/oxylipin profile (Supplementary fig. 1B). Nine free PUFA- and oxylipin species, with a variable importance projection (VIP) score

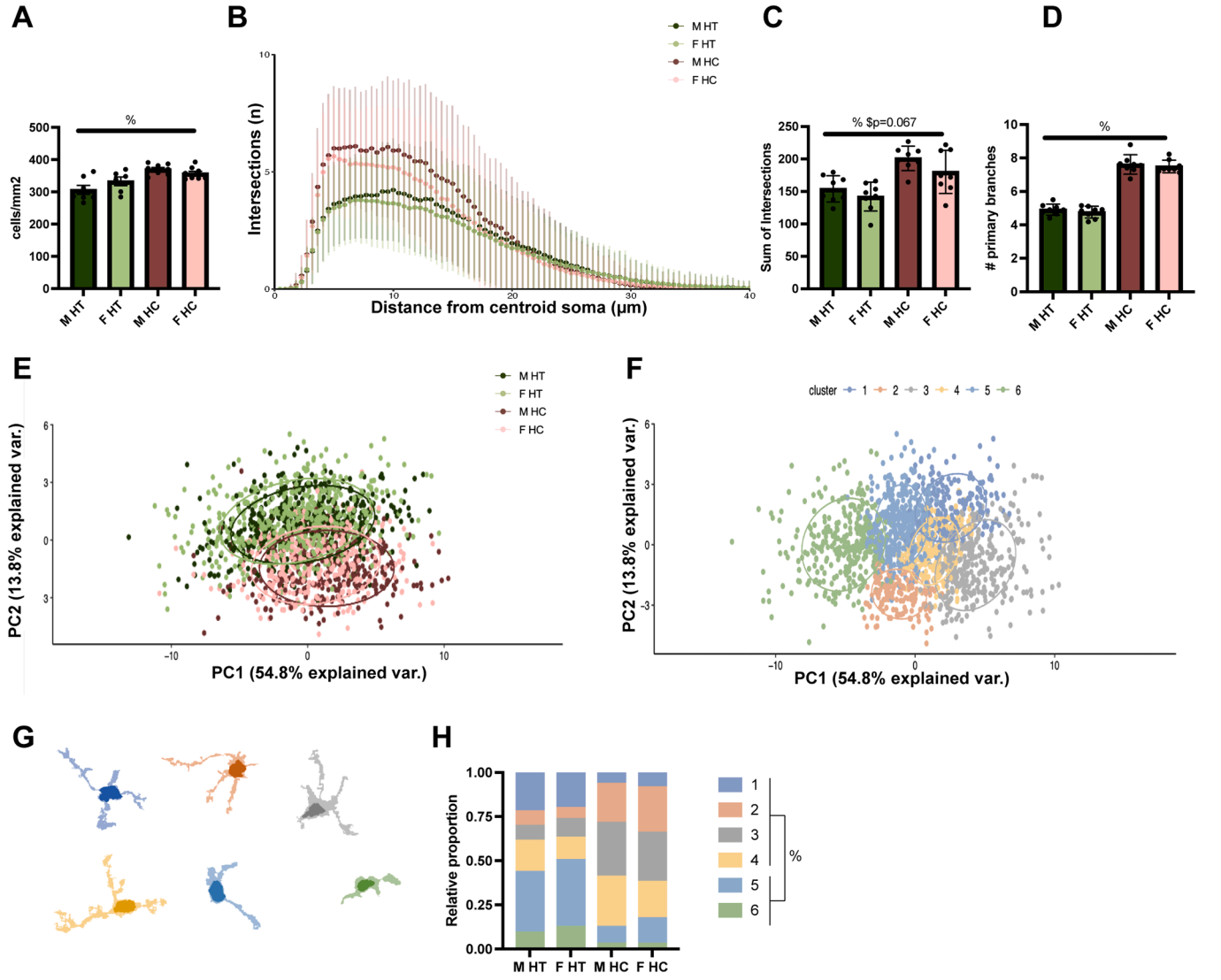

Fig. 2. Density and morphology analysis of male and female hippocampal and hypothalamic Iba1$^+$cells. A) The hippocampus (HC) presented with a higher Iba1$^+$cell density compared to the hypothalamus (HT), no sex effects. B) Sholl line plots representing complexity of cells in the hippocampus and the hypothalamus of male (M) and female (F) mice. C) Hippocampal microglia Sholl plots had a higher sum of intersections compared to hypothalamic microglia Sholl plots, no sex effects. D) Hippocampal microglia had more primary branches compared to the hypothalamus, no sex effects. E) PCA plot representing all cell coordinates (shown as dots) on the first two dimensional planes PC1/PC2. The percentage of variability retained in the respective PCs is stated between brackets on the x- and y-axes. Colors indicate experimental groups. F) PCA plot representing all cell coordinates (shown as dots) on the first two dimensional planes PC1/PC2. The percentage of variability retained in the respective PCs is stated between brackets on the x- and y-axes. Colors indicate clusters 1 to 6. G) Representative silhouette images of microglia in clusters 1 to 6, categorized per morphotype. Colors represent clusters. H) Cluster 5 and 6 were more numerous in the hypothalamus compared to the hippocampus. *N = 7–8/group. Data are presented as mean ± SD; % brain region effect; $p < 0.05$.*

higher than 1, contributed to this separation (i.e. LA, 9- and 13-hydroxyoctadecadienoic acid (HoDE), PGD_2, AA, Adrenic acid (AdA), N-6 docosapentaenoic acid (DPA N-6), 5-Oxo-eicosatetraenoic acid (5-KETE) and 5-HETE (Supplementary fig. 1C)). These results were in line with those obtained based on the PCA, indicating that in both a supervised and an unsupervised manner, we were able to separate the hypothalamus and the hippocampus based on their free PUFA/oxylipin profile. After FDR correction, α-linolenic acid (ALA), 9, 13-HoDE and LA were more abundantly present in the hypothalamus compared to the hippocampus (Fig. 1D). In the hippocampus, PUFAs such as DPA N-6, AA and other LA derivatives such as AdA, PGD_2 and 5-KETE were more abundantly present in the hippocampus (Fig. 1D, see Supplementary Table 4 for detailed statistical analyses). In order to show the detected free PUFA- and oxylipins, and to illustrate the altered free PUFA- and oxylipin species in their respective N-3 and N-6 pathways, the findings are summarized in Fig. 1E. We detected in general more N-6 PUFA pathway-derived lipid species compared to N-3 PUFA pathway-derived ones. These were also the ones mostly being different in abundance depending on brain region, with those being upregulated in the hippocampus being more downstream compared to those upregulated in the hypothalamus.

3.2. Hippocampus and hypothalamus exhibit differential microglial density and morphology, with subtle sex effects

To assess potential differences in microglia in the hippocampus and the hypothalamus in males and females, we next performed a microglial cell density and complexity analysis (i.e. unsupervised clustering of 27 microglial morphological parameters, Sholl- and fractal analyses).

3.2.1. Iba1+ cell density

we observed a higher $Iba1^+$ microglial cell density within the hippocampus compared to the hypothalamus, without sex differences (Fig. 2A, Two-way ANOVA: Brain region $F(1,25)=38,910$, $p < 0.05$; Sex: $F(1,28)=1.596$ $p = 0.217$). Iba1 coverage did not differ between brain regions or sex (Linear mixed model: Brain region $t(14) =1.20$, $p = 0.238$; Sex: $t(14) =-0.08$, $p = 0.936$). To assess potential subregional differences, we next measured $Iba1^+$ cell density in the most representative areas of these brain regions (CA and DG for the hippocampus and ARC, PVN, DM, LA and VMH for the hypothalamus). We observed no significant differences in $Iba1^+$ cell density nor coverage between males and females in the DG or the CA (Density: Supplementary fig. 2 A-B, coverage *data not shown*). Interestingly, there appeared to be a trend for a lower $Iba1^+$ cell density in females compared to males in the ARC ($p = 0.057$) (Supplementary fig. 3A). However, we observed no differences in $Iba1^+$ cell density and coverage between males and females in the PVN, DM, LH and VMH (Density: Supplementary fig. 3B-E, coverage *data not shown*).

3.2.2. Microglial complexity

Next, we extracted 1920 single-cell images of $Iba1^+$ cells. The single cell images were converted to cell silhouette images and subjected to automated skeletonization and subsequent Sholl analysis, fractal analyses and extraction of 27 morphometric features, as described before [25]. Then, a Sholl analysis was performed on these single-cell images (representative plots are shown in Fig. 2B). The sum of intersections in these plots was higher in the hippocampus compared to hypothalamus and there was a trend towards a lower sum of intersections in females (Fig. 2C Two-way ANOVA: brain region $F(1,28)=24.578$, $p < 0.01$; Sex $F(1,28)=3.631$, $p = 0.067$). In addition, the amount of primary branches (Fig. 2D) was higher in the hippocampus compared to the hypothalamus (Two-way ANOVA: brain region $F(1,28)=332.572$, $p < 0.01$; Sex $F(1,28)=0.850$, $P = 0.365$). Unsupervised clustering revealed that $Iba1^+$ cells from the hypothalamus cluster together and $Iba1^+$ cells from hippocampus cluster together, without apparent sex effects (Fig. 2E). HCPC resulted in 6 $Iba1^+$ cell clusters (Fig. 2F-G). Considering this clustering, $Iba1^+$ cells in cluster 1–4 present a more complex morphology, thus likely surveilling or homeostatic [26], while $Iba1^+$ cells in cluster 5–6 are less complex and might thus represent a more pro-inflammatory phagocytic state [27], which is why we quantified clusters 5 and 6 added together in further analysis. In the hypothalamus there were relatively more microglia in the less complex state (cluster 5–6) compared to the hippocampus. Sex did not influence the proportion of these clusters (Fig. 2H, Brain region: $F(1,28)=111.338$, $p < 0.05$; Sex: $F(1,28)= 2.517$, $p = 0.124$). To asses potential subregional effects within the hippocampus we performed a subregional complexity analysis of the DG and the CA (Supplementary fig. 2C-J). In the DG, the sum of intersections of female microglia was significantly lower than of male microglia (Supplementary fig. 2D Wilcoxon signed rank test: $W = 11$, $p < 0.05$). There were no sex differences regarding primary branching (Supplementary fig. 2E). Within the hypothalamus we analyzed specifically the ARC, PVN, DM, LH and DMH and detected no sex effects in any of the hypothalamic subregions (Supplementary fig. 3F-Y). Together these findings indicate that less $Iba1^+$ cells are present in the hypothalamus compared to the hippocampus, which seem to present a more pro-inflammatory activity state.

3.3. PUFA and oxylipin species predominantly correlate with microglial morphological parameters in the hypothalamus

To determine how the abundance of local free PUFA- and oxylipin species could be linked to microglial morphology, we next assessed potential correlations between the measured free PUFA/oxylipins and the microglial morphological parameters on which the cluster distributions are based on (Fig. 3A, B). To ease interpretation, the parameters were subdivided in three groups: related to soma-, branching- and cell properties. In general, in the hippocampus (Fig. 3A) $Iba1^+$ parameters correlated less with free PUFA- and oxylipin species compared to the hypothalamic $Iba1^+$ parameters (Fig. 3B). Interestingly, hippocampal $Iba1^+$ cell parameters correlated only to free PUFA- and oxylipin species deriving from the N-6 pathway while in the hypothalamus there were correlations between $Iba1^+$ cell parameters and free PUFA- and oxylipin species belonging to both N-3 and N-6 pathways. In both the hippocampus and the hypothalamus, branching properties and cell shape properties were correlated with PUFAs and oxylipin species, while no correlations were found with somal parameters. Interestingly in the hypothalamus, most of the detected PUFAs (ALA/GLA, eicosapentaenoic acid, DHA, LA and AA) correlated with either cell shape or branching properties and a few oxylipins correlated with these properties. AA-derived oxylipins 8- and 15-HETE negatively correlated with parameters associated with complexity. Regarding the differentially expressed PUFA and oxylipins, AA (more abundant in the hippocampus) negatively correlated with branch area and cell area. In the hypothalamus, LA and ALA were upregulated and negatively correlated with branching properties and branch- and cell perimeter, respectively. Other differentially expressed components such as PGD_2 5-KETE, DPA N-6, AdA (Hippocampus > Hypothalamus) did not correlate with any of the microglial parameters. Thus, hypothalamic microglial morphology correlated more strongly with free PUFA- and oxylipin species than hippocampal microglia, and hippocampal microglial parameters correlated only with N-6 pathway-related species as opposed to hypothalamic microglial parameters correlating with both N-3 and N-6 pathways.

4. Discussion

In this study, we investigated the potential brain region and sex differences in free PUFA- and oxylipin species, microglial morphology and how these two dimensions could possibly relate to one another. We observed clear brain region differences, in particular, PGD_2, AA, DPA N-6, AdA, 5-KETE were more abundantly present in the hippocampus, while ALA-GLA, 9- and 13-HoDE and LA were more abundantly present in the hypothalamus, without a clear sex effect. Regarding microglia,

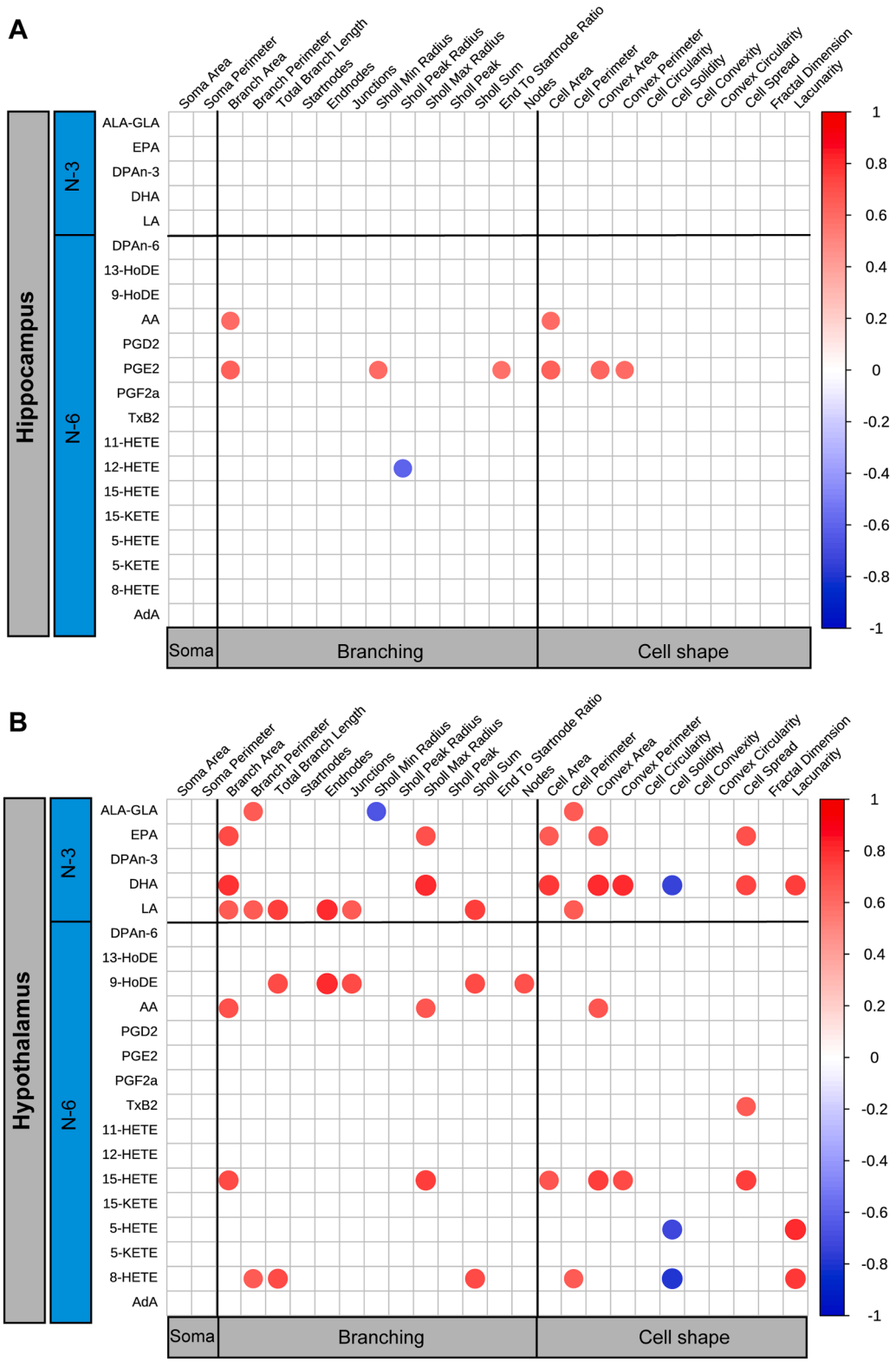

Fig. 3. Correlation of non-esterified PUFA- and oxylipin profile with microglial morphology parameters A) Hippocampal free PUFA- and oxylipin profile separated for N-3 PUFA and N-6 PUFAs correlated with hippocampal microglial parameters separated in soma, branching and cell shape characteristics. B) Hypothalamic free PUFA- and oxylipin profile separated for N-3 PUFAs and N-6 PUFAs correlated with hypothalamic microglial parameters separated in soma, branching and cell shape characteristics. *Red indicates a positive correlation, blue indicates a negative correlation, no color indicates no correlation. Correlation matrix was made without FDR-correction.*

Iba1$^+$ cell density was higher in the hippocampus compared to the hypothalamus, and these cells exhibited a higher complexity. There were subtle sex-differences in our subregional analyses: microglia derived from the DG, but not the CA of the female hippocampus were less complex compared to males. In addition, in the ARC, we observed a trend towards a higher Iba1$^+$ cell density in males compared to females. Concerning the association between free PUFA- and oxylipin species and microglia morphology, microglial parameters related to the soma did not correlate with any of the measured PUFAs and oxylipin species while branching and cell shape parameters did so across both brain regions. Microglial parameters only correlated with free PUFA- and oxylipin species from the N-6 pathway in the hippocampus while in the hypothalamus, such correlations were more profound with free PUFA- and oxylipin species from both pathways.

4.1. The hippocampus and hypothalamus exhibit differences in free PUFA/oxylipin profiles, without sex effects

Here, we detected differences in abundance of free PUFA- and oxylipin species between the hippocampus and the hypothalamus. Little is known about free PUFA- and oxylipin species within these brain regions, but previous findings support a brain regional heterogeneity in the abundance of lipid species. One study, comparing regions including the hypothalamus and the hippocampus of adult mice, reported a region-specific eicosanoid abundance, with a higher abundance of 12-HETE in the hippocampus compared to the hypothalamus [16]. This is partly in line with our findings, as we also detected different profiles between these brain regions. While we did not find differences in this specific oxylipin, this discrepancy might be due to the fact that in the aforementioned study, the authors pooled samples from different mice while we did not. Similarly, in a study in 2-month-old rats, where the free PUFA/oxylipin profile response to ischemic brain injury depended on the brain region (different for cerebellum, the hypothalamus, the cortex and the hippocampus), indicating the potential relevance of brain-region specificity [17].

Differences in membrane-bound PUFAs in brain regions, which could be a result of different amount or cell type make-up, might indirectly affect the free PUFA- and oxylipins as esterified PUFAs are metabolized from the membrane after e.g. environmental stimuli (such as inflammatory mediators) [28,29]. In the current study, the levels of free LA and ALA were lower in the hippocampus compared to the hypothalamus. This could be an effect of increased metabolization of LA-derivative (AA) and downstream AA-derivatives in the hippocampus or a higher demand or lower conversion rate for LA and ALA within the hypothalamus. Notably, the hypothalamus is highly vascularized [30] and since the circulation is the main supply of LA and ALA to the brain [3], this could contribute to the observed brain regional differences.

Compared to the hypothalamus, the abundance of oxylipins directly deriving from LA, such as 9- and 13-HoDE, appeared to be lower in the hippocampus. Whether this differential profile is contributed by a differential expression of the biosynthesizing enzymes responsible for these conversions (e.g. cyclooxygenase 1,2 and 15-lipoxygenase-1) [31,32] will need to be addressed in future studies. 9- and 13-HoDE can also be non-enzymatically oxidized by reactive oxygen species and a lower abundance of them in the hippocampus could therefore be indicative of decreased amount of ROS compared to the hypothalamus [32], potentially in line with the more homeostatic state of the microglia that we observed in the hypothalamus. Though the free PUFA- and oxylipin species that are increased in the hippocampus are N-6 PUFA derivatives, which are mostly associated with pro-inflammatory processes [33–36], we provide no evidence on the morphological level that hippocampal microglia might be in a more “pro-inflammatory“ state as a result of the increased N-6 PUFA derivatives compared to the hypothalamus. Additionally, PGD_2 has also been shown to be involved in homeostatic functions regulated by the hypothalamus, such as body temperature and hormone release [37], which could explain why its abundance in the hypothalamus is more tightly regulated (by faster metabolization or less release) compared to the hippocampus. We did detect brain region differences in microglia density and morphology, but if and how these might be affected by the local free PUFA/oxylipin profile remains to be determined. In the current study, we analyzed free PUFA- and oxylipin species in homeostatic conditions, but we have shown before that free PUFA- and oxylipin species levels are altered in response to early-life stress, diet and lipopolysaccharide stimulus in the hypothalamus [38], indicating that these measures are sensitive and dynamically adapt to such external stimuli. Given the current baseline differences between the two regions, it is plausible that the free PUFA/oxylipin profile might also differentially respond to stimuli.

We did not detect any sex differences in free PUFA- and oxylipin species in either of the brain regions. In line with our findings, the free PUFA/oxylipin profiles of male and female 1-day old rat pups were similar [18]. In contrast, the cerebellum of 4-month-old mice exhibited sex differences, with 5-HETE and 5-HEPE being higher in males than in females [19] and similarly, 32-week-old mice males exhibited higher levels of 9-HETE, 11-HETE, and 15-HETE in a whole hemisphere compared to females [20] and there is evidence that in a mouse model for accelerated aging, the cortex contained higher levels of LA and AA-derived oxylipins [39], possibly contributing to increased neuroinflammation associated with aging [40,41]. Discrepancies between these findings and our observations might be due to the specific brain regions addressed in our study versus those reported earlier, or might be age-dependent, as sex differences have not been described until 4 months of age. While most of these measures are under homeostatic conditions, potential sex differences in free PUFA/oxylipin profile might become more apparent in neuroinflammatory conditions. Indeed, there is evidence that male and female patients with multiple sclerosis, a disease with a strong neuroinflammatory component and a sex-specific vulnerability [42], exhibit a sex-specific free PUFA/oxylipin profile in the cerebrospinal fluid [43]. The origin of such sex-specific effects on free PUFA- and oxylipin species at different ages remains to be understood, but it could be due to a different free PUFA- and oxylipin metabolism in the periphery. For example, there is evidence from humans that plasma and blood cell concentrations of PUFAs [44] are sex- and age-dependent.

4.2. Microglial parameters in the hippocampus and hypothalamus reveals regional differences and sex-dependent differences specifically in the hippocampal DG and arcuate nucleus of the hypothalamus

We observed that the hippocampus was more densely populated by microglia, and additionally exhibited a higher microglial complexity compared to the hypothalamus. Few studies have investigated glial cell density in the hypothalamus (systematically reviewed in [45]). A higher glial cell density was found in the hippocampus compared to the hypothalamus [46,47], but no distinctions are made between microglia and astrocytes, so a direct comparison is not possible. Though a higher Iba1$^+$ density is mostly associated with a pro-inflammatory state in neurodegenerative and neuropsychiatric disorders such as AD [48] and MDD [4] respectively, the effect of a brain-region difference in cell density in the homeostatic brain is unknown. The findings regarding complexity suggest that hypothalamic and hippocampal microglia might be in a different activity state during homeostasis, partly due to their localization in the brain. In fact, the hypothalamus, due to its ventral positioning, is highly vascularized and might thus be more abundantly exposed to circulating cues and metabolites [30], potentially influencing their activity state with a less complex morphology. In addition, there is evidence that microglia in the midbrain (including the hypothalamus) express lower levels of homeostatic microglial proteins [49,50] such as triggering receptor expressed on myeloid cells-2 and purinergic receptor P2RY12, compared to the hippocampus [49].

Subtle microglial sex differences were uncovered after subregional analyses. Most studies focusing on sex differences in the hypothalamus

are in the context of feeding behavior and obesity. One study investigated microglia in the context of a high-fat high-sugar diet and found no sex differences in their complexity in control animals, in line with our findings [51]. However, comparative studies on hippocampal microglia in males and females indicate age-dependent sex-specific differences [15]. In adulthood, females exhibit more ''pro-inflammatory'' microglia compared to males [52], contrasting with findings during development [12]. Transcriptomic analyses revealed divergent developmental trajectories, with male microglial development plateauing earlier than females [52,53], leading to sex-differences in complexity, and Iba1 density in adulthood [14,52]. Taken together, these studies suggest a sex-related heterogeneity in microglia. Notably, most earlier studies rely on a cruder analysis of microglial complexity. Two more recent studies, including several brain regions but not the hypothalamus reported no sex differences in any of these properties using the same unbiased semi-automated and more detailed morphological analyses [13,25] as used here. We cannot exclude that more prominent sex differences appear in areas of the hypothalamus that we did not currently sample, such as in the preoptic area where sex-differences have been described in rats [54] or upon stimuli. Regarding the hippocampus, using the same method as in the current study, it has been proposed before that there were no sex differences in microglial morphology and density in the DG and the CA [25], which partly is in line with our findings, except that we showed a decreased microglial complexity in the DG in females. Compared to our study, it is noteworthy that in this study [25], more brain regions were compared, possibly affecting the outcome. This suggest that the method used to sample (single-cell silhouettes thresholding vs full image thresholding) and to analyze microglia morphology (based on visual inspection vs unbiased), as well as the precision in subregional analyses are key to capture more subtle brain region- and sex-dependent microglial heterogeneity. Finally, as discussed for the free PUFA- and oxylipin profile, larger sex differences might become apparent in less homeostatic systems. Indeed, after stress (16–20 weeks of age), microglia were less complex in adult female, but not male mice [55].

4.3. PUFA and oxylipin species predominantly correlate with microglial parameters in the hypothalamus

Regarding the potential relationship between the differences in Iba1$^+$ morphological parameters and the abundance of free PUFA- and oxylipin species in the microenvironment of the brain regions, we observed, in general, that hypothalamic Iba1$^+$cells cell parameters correlated more strongly to free PUFA- and oxylipin species than hippocampal ones, with hypothalamic microglial parameters correlating with free PUFA- and oxylipin species from both the N-3 and N-6 pathways, while these correlations only occurred with PUFA and oxylipins in the N-6 pathway in hippocampus. These observations suggest that hypothalamic microglia might be more sensitive to the local free PUFA/oxylipin profile compared to hippocampal microglia. The inverse correlation of microglial parameters associated with high complexity (such as branching area) with the pathway that converts AA into PGE_2 could be of specific interest, as the other AA metabolization pathways that are upregulated (e.g. AdA and 5-KETE) in the hippocampus do not correlate with any parameters. The relationship between microglia activity state/morphology and free PUFA- and oxylipin species abundance remains complex. Microglia are responsive to free PUFA- and oxylipins, but might also play a role in their abundance via lipid biosynthesis for auto- or paracrine signaling [56–58]. This study lacks cell-specific resolution for the free PUFA- and oxylipin profiling, so the observed effects might derive from other cells within the assessed brain regions (such as neurons, or astrocytes). To address this, studies investigating the release of free PUFA- and oxylipin species and the expression of enzymes responsible for metabolizing PUFAs to oxylipins on a cell-specific level will be of interest for further research. In addition, it would be interesting to build further on this work and study the effect of the relationship between PUFAs or oxylipin milieu on microglial phenotype and function.

5. Conclusion

We observed brain region-dependent free PUFA/oxylipin profile and microglia heterogeneity as well as a distinct association between free PUFA- and oxylipin species and microglia morphology, particularly in the hypothalamus. Our study contributes to the understanding of free PUFA- and oxylipin species and their relationship with neuroinflammatory processes in the homeostatic brain, providing new avenues for studying the role of free PUFA- and oxylipin species, microglia and their interaction in the context of neuropsychiatric and neurodegenerative disorders.

Availability of data and materials

The data that support the findings of this study are available from the corresponding author upon reasonable request.

Funding

This work was supported by a grant from the Dutch Research Council (NWO Vidi grant 91,719,305 to GK) and a grant from Amsterdam Neuroscience (NDIS-2019–01 to GK).

CRediT authorship contribution statement

J. Geertsema: Writing – review & editing, Writing – original draft, Visualization, Methodology, Investigation, Formal analysis, Data curation, Conceptualization. **M.A. Franßen:** Writing – review & editing, Visualization, Methodology, Investigation, Formal analysis, Data curation. **F. Barban:** Investigation, Data curation. **L. Šarauskytė:** Investigation, Data curation. **M. Giera:** Resources. **G. Kooij:** Writing – review & editing, Supervision, Funding acquisition, Conceptualization. **A Korosi:** Writing – review & editing, Writing – original draft, Supervision, Funding acquisition, Conceptualization.

Declaration of competing interest

None.

Acknowledgements

The authors would like to thank H. van Weering for assistance with the morphometric analyses.

Supplementary materials

Supplementary material associated with this article can be found, in the online version, at doi:10.1016/j.plefa.2024.102662.

References

[1] X. Zhao, S. Zhang, A.R. Sanders, J. Duan, Brain lipids and lipid droplet dysregulation in Alzheimer's disease and neuropsychiatric disorders, Complex. Psychiatry 9 (2023) 154–171, https://doi.org/10.1159/000535131.
[2] S.Y. Cheon, Impaired cholesterol metabolism, neurons, and neuropsychiatric disorders, Exp. Neurobiol. 32 (2023) 57–67, https://doi.org/10.5607/en23010.
[3] R.P. Bazinet, S. Layé, Polyunsaturated fatty acids and their metabolites in brain function and disease, Nat. Rev. Neurosci. 15 (2014) 771–785, https://doi.org/10.1038/nrn3820.
[4] H. Zhu, A. Guan, J. Liu, L. Peng, Z. Zhang, S. Wang, Noteworthy perspectives on microglia in neuropsychiatric disorders, J. Neuroinflammation. 20 (2023) 223, https://doi.org/10.1186/s12974-023-02901-y.
[5] Y. Wang, L. Dong, D. Pan, D. Xu, Y. Lu, S. Yin, et al., Effect of high ratio of n-6/n-3 PUFAs on depression: a meta-analysis of prospective studies, Front. Nutr. 9 (2022), https://doi.org/10.3389/fnut.2022.889576.

[6] R. Baccouch, Y. Shi, E. Vernay, M. Mathelié-Guinlet, N. Taib-Maamar, S. Villette, et al., The impact of lipid polyunsaturation on the physical and mechanical properties of lipid membranes, Biochimica et Biophysica Acta (BBA) - Biomembranes 1865 (2023) 184084, https://doi.org/10.1016/j.bbamem.2022.184084.
[7] C.N. Serhan, N. Chiang, J. Dalli, The resolution code of acute inflammation: novel pro-resolving lipid mediators in resolution, Semin. Immunol. 27 (2015) 200–215, https://doi.org/10.1016/j.smim.2015.03.004.
[8] C. Rey, J.C. Delpech, C. Madore, A. Nadjar, A.D. Greenhalgh, C. Amadieu, et al., Dietary n-3 long chain PUFA supplementation promotes a pro-resolving oxylipin profile in the brain, Brain Behav. Immun. (2019), https://doi.org/10.1016/j.bbi.2018.07.025.
[9] A. Nadjar, Q. Leyrolle, C. Joffre, S. Laye, Bioactive lipids as new class of microglial modulators: when nutrition meets neuroimunology, Prog. Neuropsychopharmacol. Biol. Psychiatry 79 (2017) 19–26, https://doi.org/10.1016/j.pnpbp.2016.07.004.
[10] J.Y. Bang, J. Zhao, M. Rahman, S. St-Cyr, P.O. McGowan, J.C. Kim, Hippocampus-anterior hypothalamic circuit modulates stress-induced endocrine and behavioral response, Front. Neural Circuits. 16 (2022) 894722, https://doi.org/10.3389/fncir.2022.894722.
[11] D.A. Bangasser, R.J. Valentino, Sex differences in stress-related psychiatric disorders: neurobiological perspectives, Front. Neuroendocrinol. 35 (2014) 303–319, https://doi.org/10.1016/j.yfrne.2014.03.008.
[12] N. Yanguas-Casás, Physiological sex differences in microglia and their relevance in neurological disorders, Neuroimmunol. Neuroinflamm. (2020), https://doi.org/10.20517/2347-8659.2019.31.
[13] G. Colombo, R.J.A. Cubero, L. Kanari, A. Venturino, R. Schulz, M. Scolamiero, et al., A tool for mapping microglial morphology, morphOMICs, reveals brain-region and sex-dependent phenotypes, Nat. Neurosci. 25 (2022) 1379–1393, https://doi.org/10.1038/s41593-022-01167-6.
[14] D. Guneykaya, A. Ivanov, D.P. Hernandez, V. Haage, B. Wojtas, N. Meyer, et al., Transcriptional and translational differences of microglia from male and female brains, Cell Rep. 24 (2018) 2773–2783, https://doi.org/10.1016/j.celrep.2018.08.001, e6.
[15] J. Han, Y. Fan, K. Zhou, K. Blomgren, R.A. Harris, Uncovering sex differences of rodent microglia, J. Neuroinflammation. 18 (2021) 74, https://doi.org/10.1186/s12974-021-02124-z.
[16] M. Reinicke, J. Dorow, K. Bischof, J. Leyh, I. Bechmann, U. Ceglarek, Tissue pretreatment for LC-MS/MS analysis of PUFA and eicosanoid distribution in mouse brain and liver, Anal. Bioanal. Chem. 412 (2020) 2211–2223, https://doi.org/10.1007/s00216-019-02170-w.
[17] M. Hennebelle, Z. Zhang, A.H. Metherel, A.P. Kitson, Y. Otoki, C.E. Richardson, et al., Linoleic acid participates in the response to ischemic brain injury through oxidized metabolites that regulate neurotransmission, Sci. Rep. 7 (2017) 4342, https://doi.org/10.1038/s41598-017-02914-7.
[18] M. Hennebelle, R.K. Morgan, S. Sethi, Z. Zhang, H. Chen, A.C. Grodzki, et al., Linoleic acid-derived metabolites constitute the majority of oxylipins in the rat pup brain and stimulate axonal growth in primary rat cortical neuron-glia co-cultures in a sex-dependent manner, J. Neurochem. 152 (2020) 195–207, https://doi.org/10.1111/jnc.14818.
[19] A.Y. Taha, Á. Gaudioso, M. Moran-Garrido, S.M. Camunas-Alberca, J. Bachiller-Hernández, J. Sáiz, et al., Neurons regulate the esterification of bioactive lipid mediators in the brain of acid sphingomyelinase deficient mice, Prog. Neuropsychopharmacol. Biol. Psychiatry 129 (2024) 110896, https://doi.org/10.1016/j.pnpbp.2023.110896.
[20] J.E. Norman, S. Nuthikattu, D. Milenkovic, J.C. Rutledge, A.C. Villablanca, Sex-specific response of the brain free oxylipin profile to soluble epoxide hydrolase inhibition, Nutrients. 15 (2023), https://doi.org/10.3390/nu15051214.
[21] E. Gart, K. Salic, M. Morrison, M. Caspers, W. van Duyvenvoorde, M. Heijnk, et al., Krill oil treatment increases distinct pufas and oxylipins in adipose tissue and liver and attenuates obesity-associated inflammation via direct and indirect mechanisms, Nutrients. 13 (2021) 2836, https://doi.org/10.3390/nu13082836.
[22] S. Bijlsma, I. Bobeldijk, E.R. Verheij, R. Ramaker, S. Kochhar, I.A. Macdonald, et al., Large-scale human metabolomics studies: a strategy for data (pre-) processing and validation, Anal. Chem. 78 (2006) 567–574, https://doi.org/10.1021/ac051495j.
[23] R. Wei, J. Wang, M. Su, E. Jia, S. Chen, T. Chen, et al., Missing value imputation approach for mass spectrometry-based metabolomics data, Sci. Rep. 8 (2018) 663, https://doi.org/10.1038/s41598-017-19120-0.
[24] J.R. Bourgeois, G. Kalyanasundaram, C. Figueroa, A. Srinivasan, A.M. Kopec, A semi-automated brain atlas-based analysis pipeline for c-Fos immunohistochemical data, J. Neurosci. Methods 348 (2021) 108982, https://doi.org/10.1016/j.jneumeth.2020.108982.
[25] H.R.J. van Weering, T.W. Nijboer, M.L. Brummer, E.W.G.M. Boddeke, B.J.L. Eggen, Microglia morphotyping in the adult mouse <scp>CNS</scp>using hierarchical clustering on principal components reveals regional heterogeneity but no sexual dimorphism, Glia 71 (2023) 2356–2371, https://doi.org/10.1002/glia.24427.
[26] M.-È. Tremblay, B. Stevens, A. Sierra, H. Wake, A. Bessis, A. Nimmerjahn, The role of microglia in the healthy brain, J. Neurosci. 31 (2011) 16064–16069, https://doi.org/10.1523/JNEUROSCI.4158-11.2011.
[27] J. Leyh, S. Paeschke, B. Mages, D. Michalski, M. Nowicki, I. Bechmann, et al., Classification of microglial morphological phenotypes using machine learning, Front. Cell Neurosci. 15 (2021) 701673, https://doi.org/10.3389/fncel.2021.701673.
[28] Y. Xiao, Y. Huang, Z.-Y. Chen, Distribution, depletion and recovery of docosahexaenoic acid are region-specific in rat brain, Br. J. Nutr. 94 (2005) 544–550, https://doi.org/10.1079/BJN20051539.
[29] H. Zhang, Y. He, C. Song, Z. Chai, C. Liu, S. Sun, et al., Analysis of fatty acid composition and sensitivity to dietary n-3 PUFA intervention of mouse n-3 PUFA-enriched tissues/organs, Prostaglandins. Leukot. Essent. Fatty. Acids. 192 (2023) 102568, https://doi.org/10.1016/j.plefa.2023.102568.
[30] R.E. Henn, K. Guo, S.E. Elzinga, M.H. Noureldein, F.E. Mendelson, J.M. Hayes, et al., Single-cell RNA sequencing identifies hippocampal microglial dysregulation in diet-induced obesity, iScience 26 (2023) 106164, https://doi.org/10.1016/j.isci.2023.106164.
[31] L.H. Shinto, J. Raber, A. Mishra, N. Roese, L.C. Silbert, A review of oxylipins in Alzheimer's disease and related dementias (ADRD): potential therapeutic targets for the modulation of vascular tone and inflammation, Metabolites. 12 (2022) 826, https://doi.org/10.3390/metabo12090826.
[32] M. Szczuko, D. Kotlęga, J. Palma, A. Zembroń-Łacny, A. Tylutka, M. Gołąb-Janowska, et al., Lipoxins, RevD1 and 9, 13 HODE as the most important derivatives after an early incident of ischemic stroke, Sci. Rep. 10 (2020) 12849, https://doi.org/10.1038/s41598-020-69831-0.
[33] Q.-L. Ma, C. Zhu, M. Morselli, T. Su, M. Pelligrini, Z. Lu, et al., The novel omega-6 fatty acid docosapentaenoic acid positively modulates brain innate immune response for resolving neuroinflammation at early and late stages of humanized APOE-based Alzheimer's disease models, Front. Immunol. 11 (2020) 558036, https://doi.org/10.3389/fimmu.2020.558036.
[34] H. Brouwers, H. Jonasdottir, J. Kwekkeboom, C. Lopez-Vicario, J. Claria, J. Freysdottir, et al., Adrenic acid as a novel anti-inflammatory player in osteoarthritis, OsteoArthritis Cartilage 26 (2018) S126, https://doi.org/10.1016/j.joca.2018.02.274.
[35] C. Corwin, A. Nikolopoulou, A.L. Pan, M. Nunez-Santos, S. Vallabhajosula, P. Serrano, et al., Prostaglandin D2/J2 signaling pathway in a rat model of neuroinflammation displaying progressive parkinsonian-like pathology: potential novel therapeutic targets, J. Neuroinflammation. 15 (2018) 272, https://doi.org/10.1186/s12974-018-1305-3.
[36] C.N. Serhan, N. Chiang, T.E. Van Dyke, Resolving inflammation: dual anti-inflammatory and pro-resolution lipid mediators, Nat. Rev. Immunol. 8 (2008) 349–361, https://doi.org/10.1038/nri2294.
[37] M. Joo, R.T. Sadikot, PGD synthase and PGD2 in immune resposne, Mediators. Inflamm. 2012 (2012) 503128, https://doi.org/10.1155/2012/503128.
[38] Reemst K., Broos J.Y., Abbink M.R., Cimetti C., Giera M., Kooij G., et al. Early-life stress and dietary fatty acids impact the brain lipid/oxylipin profile into adulthood, basally and in response to LPS. Front. Immunol. 2022;13. ARTN 967437 10.3389/fimmu.2022.967437.
[39] A. Currais, J. Goldberg, C. Farrokhi, M. Chang, M. Prior, R. Dargusch, et al., A comprehensive multiomics approach toward understanding the relationship between aging and dementia, Aging (Albany. NY) 7 (2015) 937–955, https://doi.org/10.18632/aging.100838.
[40] X. Li, C. Li, W. Zhang, Y. Wang, P. Qian, H. Huang, Inflammation and aging: signaling pathways and intervention therapies, Signal. Transduct. Target. Ther. 8 (2023) 239, https://doi.org/10.1038/s41392-023-01502-8.
[41] C. Joffre, C. Rey, S. Layé, N-3 Polyunsaturated Fatty Acids and the Resolution of Neuroinflammation, Front. Pharmacol. 10 (2019) 1022, https://doi.org/10.3389/fphar.2019.01022.
[42] N. Alvarez-Sanchez, S.E. Dunn, Potential biological contributers to the sex difference in multiple sclerosis progression, Front. Immunol. 14 (2023) 1175874, https://doi.org/10.3389/fimmu.2023.1175874.
[43] I. Håkansson, S. Gouveia-Figueira, J. Ernerudh, M. Vrethem, N. Ghafouri, B. Ghafouri, et al., Oxylipins in cerebrospinal fluid in clinically isolated syndrome and relapsing remitting multiple sclerosis, Prostaglandins. Other Lipid Mediat. 138 (2018) 41–47, https://doi.org/10.1016/j.prostaglandins.2018.08.003.
[44] S. Lohner, K. Fekete, T. Marosvölgyi, T. Decsi, Gender differences in the long-chain polyunsaturated fatty acid status: systematic review of 51 publications, Ann. Nutr. Metab. 62 (2013) 98–112, https://doi.org/10.1159/000345599.
[45] D. Keller, C. Erö, H. Markram, Cell Densities in the Mouse Brain: a Systematic Review, Front. Neuroanat. 12 (2018), https://doi.org/10.3389/fnana.2018.00083.
[46] L.J. Lawson, V.H. Perry, P. Dri, S. Gordon, Heterogeneity in the distribution and morphology of microglia in the normal adult mouse brain, Neuroscience 39 (1990) 151–170, https://doi.org/10.1016/0306-4522(90)90229-w.
[47] V.L. Savchenko, J.A. McKanna, I.R. Nikonenko, G.G. Skibo, Microglia and astrocytes in the adult rat brain: comparative immunocytochemical analysis demonstrates the efficacy of lipocortin 1 immunoreactivity, Neuroscience 96 (2000) 195–203, https://doi.org/10.1016/s0306-4522(99)00538-2.
[48] C. Gao, J. Jiang, Y. Tan, S. Chen, Microglia in neurodegenerative diseases: mechanism and potential therapeutic targets, Signal. Transduct. Target. Ther. 8 (2023) 359, https://doi.org/10.1038/s41392-023-01588-0.
[49] C.D. Schmid, L.N. Sautkulis, P.E. Danielson, J. Cooper, K.W. Hasel, B.S. Hilbush, et al., Heterogeneous expression of the triggering receptor expressed on myeloid cells-2 on adult murine microglia, J. Neurochem. 83 (2002) 1309–1320, https://doi.org/10.1046/j.1471-4159.2002.01243.x.
[50] S.E. Haynes, G. Hollopeter, G. Yang, D. Kurpius, M.E. Dailey, W.-B. Gan, et al., The P2Y12 receptor regulates microglial activation by extracellular nucleotides, Nat. Neurosci. 9 (2006) 1512–1519, https://doi.org/10.1038/nn1805.
[51] C.M. Daly, J. Saxena, J. Singh, M.R. Bullard, E.O. Bondy, A. Saxena, et al., Sex differences in response to a high fat, high sucrose diet in both the gut microbiome and hypothalamic astrocytes and microglia, Nutr. Neurosci. 25 (2022) 321–335, https://doi.org/10.1080/1028415X.2020.1752996.
[52] J.M. Schwarz, P.W. Sholar, S.D. Bilbo, Sex differences in microglial colonization of the developing rat brain, J. Neurochem. 120 (2012) 948–963, https://doi.org/10.1111/j.1471-4159.2011.07630.x.

[53] R. Hanamsagar, M.D. Alter, C.S. Block, H. Sullivan, J.L. Bolton, S.D. Bilbo, Generation of a microglial developmental index in mice and in humans reveals a sex difference in maturation and immune reactivity, Glia 65 (2017) 1504–1520, https://doi.org/10.1002/glia.23176.

[54] K.M. Lenz, B.M. Nugent, R. Haliyur, M.M. McCarthy, Microglia are essential to masculinization of brain and behavior, J. Neurosci. 33 (2013) 2761–2772, https://doi.org/10.1523/JNEUROSCI.1268-12.2013.

[55] M. Tsyglakova, A.M. Huskey, E.H. Hurst, N.M. Telep, M.C. Wilding, M. E. Babington, et al., Sex and region-specific effects of variable stress on microglia morphology, Brain Behav. Immun. Health 18 (2021) 100378, https://doi.org/10.1016/j.bbih.2021.100378.

[56] D. Rademacher, Production of hydroxyeicosatetraenoic acids and prostaglandins by a novel rat microglial cell line, J. Neuroimmunol. 149 (2004) 130–141, https://doi.org/10.1016/j.jneuroim.2003.12.022.

[57] K. Iwasa, S. Yamamoto, K. Yamashina, N. Yagishita-Kyo, K. Maruyama, T. Awaji, et al., A peripheral lipid sensor GPR120 remotely contributes to suppression of PGD2-microglia-provoked neuroinflammation and neurodegeneration in the mouse hippocampus, J. Neuroinflammation. 18 (2021) 304, https://doi.org/10.1186/s12974-021-02361-2.

[58] C. Madore, Q. Leyrolle, L. Morel, M. Rossitto, A.D. Greenhalgh, J.C. Delpech, et al., Essential omega-3 fatty acids tune microglial phagocytosis of synaptic elements in the mouse developing brain, Nat. Commun. 11 (2020) 6133, https://doi.org/10.1038/s41467-020-19861-z.